

University of Nebraska - Lincoln

DigitalCommons@University of Nebraska - Lincoln

Publications from USDA-ARS / UNL Faculty

U.S. Department of Agriculture: Agricultural
Research Service, Lincoln, Nebraska

2009

A WEIGHING LYSIMETER FOR CROP WATER USE DETERMINATION IN THE JORDAN VALLEY, JORDAN

Steven R. Evett

USDA-ARS, steve.evett@ars.usda.gov

Naem T. Mazahrih

National Center for Agricultural Research and Extension

Mohammed A. Jitan

National Center for Agricultural Research and Extension

Mahmoud H. Sawalha

National Center for Agricultural Research and Extension

Paul D. Colaizzi

USDA-ARS, Paul.Colaizzi@ARS.USDA.GOV

See next page for additional authors

Follow this and additional works at: <https://digitalcommons.unl.edu/usdaarsfacpub>

Evett, Steven R.; Mazahrih, Naem T.; Jitan, Mohammed A.; Sawalha, Mahmoud H.; Colaizzi, Paul D.; and Ayars, James E., "A WEIGHING LYSIMETER FOR CROP WATER USE DETERMINATION IN THE JORDAN VALLEY, JORDAN" (2009). *Publications from USDA-ARS / UNL Faculty*. 1813.
<https://digitalcommons.unl.edu/usdaarsfacpub/1813>

This Article is brought to you for free and open access by the U.S. Department of Agriculture: Agricultural Research Service, Lincoln, Nebraska at DigitalCommons@University of Nebraska - Lincoln. It has been accepted for inclusion in Publications from USDA-ARS / UNL Faculty by an authorized administrator of DigitalCommons@University of Nebraska - Lincoln.

Authors

Steven R. Evett, Naem T. Mazahrih, Mohammed A. Jitan, Mahmoud H. Sawalha, Paul D. Colaizzi, and James E. Ayars

A WEIGHING LYSIMETER FOR CROP WATER USE DETERMINATION IN THE JORDAN VALLEY, JORDAN

S. R. Evett, N. T. Mazahrih, M. A. Jitan, M. H. Sawalha, P. D. Colaizzi, J. E. Ayars

ABSTRACT. Efficiency of water use in irrigated agriculture can be improved by providing irrigation scheduling information to farmers. Since 2003, the Middle Eastern Regional Irrigation Management Information Systems (MERIMIS) project has focused on improving irrigation scheduling in Jordan, Palestine, and Israel with cooperators from the region and the U.S. Their efforts have established a network of 15 weather stations to support an irrigation scheduling service using the paradigm that crop water use is equal to a reference evapotranspiration (ET_r) value (calculated from weather data) multiplied by a crop coefficient. Because crop coefficients developed in one region often do not transfer exactly to another region, crop coefficient values should be developed for those crops commonly grown in the Middle Eastern region and for the agronomic practices, including row spacings, prevalent in the region. Row spacings in this region are often wider than in other regions so that full canopy cover is often not attained, and spacings vary among farmers, leading to an important crop cover factor influence on ET rates throughout the growing season. This article describes the site selection, design, construction, calibration, and preliminary results for a weighing lysimeter built by the MERIMIS team for determination of crop coefficients in the Jordan Valley. Distinct features of the design include the low roof that guarantees at least 1.5 m of soil depth all around the lysimeter, the tall scale-support piers that allow for suspension of the vacuum drainage tanks from the scale so that drainage does not change lysimeter mass, the elevated load cell and datalogger that provide insurance against the unlikely event of flooding, and the rectangular surface that accommodates the wide variety of row spacings used in the Jordan Valley. The lysimeter is sited in the center of a 100×200 m drip irrigated field, is 2.4×3 m in surface area and 2.5 m deep, and has a calibrated accuracy of 0.11 mm of water and resolution of 0.064 mm. Preliminary data show that the lysimeter and associated weather instrumentation are working as expected and are able to detect half-hourly ET rate responses.

Keywords. Crop coefficient, Crop water use, Evapotranspiration, Water use efficiency, Weighing lysimeter.

Irrigators need accurate and timely information on when and how much water to apply, but few farmers in the Middle East have the tools needed to make these irrigation scheduling decisions in the best way to obtain high yields and crop quality while conserving water. Since 2003, a regional project has focused on improving irrigation scheduling in Jordan, Palestine, and Israel. The Middle Eastern Regional Irrigation Management Information Systems (MERIMIS) project involves cooperators from Palestine, Jordan, Israel, and the U.S., all working on various aspects of irrigation scheduling. Some of the work involves irrigation

trials at specific locations and with specific crops (e.g., cucumber, olive, onion, date palm, almonds, etc.), and some work involves installation and operation of a weather station network that provides the basic weather data needed for crop water use estimation. So far, there are 15 weather stations in Jordan, Palestine, and Israel combined. Each station measures wind speed, air humidity and temperature, and solar irradiance, i.e., the four weather conditions that influence how much water is used by crops.

Crop water use estimation from weather data requires knowledge of two factors: the reference evapotranspiration (ET_r = reference crop water use), which can be calculated from the weather data, and a factor called the crop coefficient (K_c). The crop water use, symbolized by ET_c , is estimated as:

$$ET_c = K_c \times ET_r \quad (1)$$

Values of K_c increase as a crop grows, reach a plateau at full crop cover, and decrease as the crop senesces or matures. For a particular crop, values of K_c are influenced by row spacing and crop cover factor. Unfortunately, specific values of K_c are not well known for the Middle East, particularly for the Jordan Valley, which contains most of the irrigated land in Jordan (750 km^2) and is more than 200 m below sea level. At this time, the MERIMIS project team members are relying on values of K_c from international publications such as United Nations FAO publication 56 (Allen et al., 1998), which assembles K_c values from many regions of the earth but is heavily weighted to those areas with a long history of strong agricultural science.

Submitted for review in October 2008 as manuscript number SW 7758; approved for publication by the Soil & Water Division of ASABE in January 2009.

Mention of trade names or commercial products in this article is solely for the purpose of providing specific information and does not imply recommendation or endorsement by the USDA.

The authors are **Steven R. Evett, ASABE Member**, Research Soil Scientist, USDA-ARS Conservation and Production Research Laboratory, Bushland, Texas; **Naem Th. Mazahrih**, Soil Scientist, **Mohammed A. Jitan**, Agricultural Engineer, and **Mahmoud H. Sawalha**, Mechanical Engineer, National Center for Agricultural Research and Extension, Baq'a, Jordan; **Paul D. Colaizzi, ASABE Member Engineer**, Agricultural Engineer, USDA-ARS Conservation and Production Research Laboratory, Bushland, Texas; and **James E. Ayars, ASABE Member Engineer**, Agricultural Engineer, USDA-ARS Water Management Research Laboratory, Parlier, California. **Corresponding author:** Steven R. Evett, USDA-ARS Conservation and Production Research Laboratory, P.O. Drawer 10, Bushland, TX 79012; phone: 806-356-5775; fax: 806-356-5750; e-mail: Steve.Evett@ars.usda.gov.

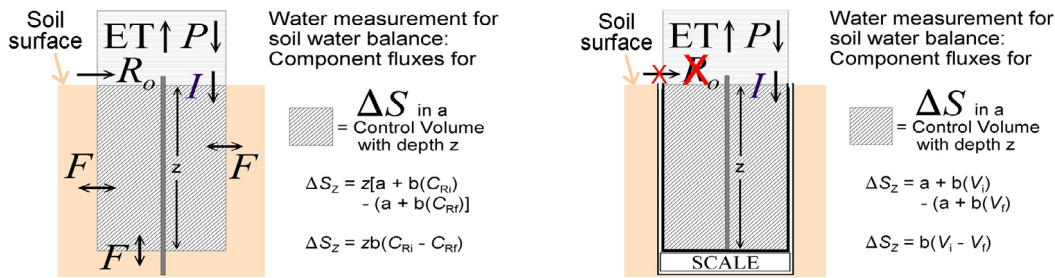


Figure 1. Control of water fluxes into and out of a soil prism called the control volume (left) is simplified with a weighing lysimeter (right). Most runoff and evaporation are eliminated by the freeboard of the top edges of the soil tank and the outer enclosure. Lateral and vertical soil water fluxes are completely controlled except at the soil surface. The change in storage (ΔS), which must be calculated from soil water content determinations (usually from calibration equations such as those shown at left) is determined by changes in lysimeter mass determined with a scale (right). The calibration equation shown has intercept a , slope b , and measured variable C_R , which for the neutron moisture meter would be the count ratio and which is measured at an initial time (C_{Ri}) and a final time (C_{Rf}). Over this time period, the change in stored soil water (ΔS_z , depth units) in a control volume of depth z is calculated by multiplying z times the difference in water contents, showing that only the slope term affects the accuracy of calculating stored soil water.

Unfortunately, crop coefficients developed in one region often do not transfer exactly to another region; thus, crop coefficient values should be developed for those crops commonly grown in the Middle Eastern region and for the agronomic practices, including row spacings, prevalent in the region. Row spacing is often wider in this region than in other regions such that full canopy cover is often not attained, and the crop cover factor influences ET rates throughout the growing season. To determine K_c , crop water use and the weather must be measured simultaneously so that the K_c values over the cropping season can be calculated from:

$$K_c = ET_{cm}/ET_r \quad (2)$$

where ET_{cm} is measured crop water use.

All measurements of crop water use depend on knowledge of the soil water balance from which ET_{cm} is calculated:

$$ET_{cm} = P + I - R - F - \Delta S \quad (3)$$

where P is precipitation depth, I is irrigation depth, R is the depth of runoff, F is the depth of water lost to deep percolation below the root zone or gained by upward flow from a shallow aquifer or deeper soil horizons, and ΔS is the change in the depth of water stored in the soil due to crop water use, irrigation, precipitation, runoff, and/or deep percolation (fig. 1, left) with all terms expressed in depth units (often mm) per unit time. While measurements of rainfall and irrigation depths are possible with rain gauges and water meters, it is difficult to measure the change in storage of soil water or the loss of water to deep percolation. Fortunately, these two measurements can be made very accurately with a weighing lysimeter because the soil container prevents loss of water to deep percolation (and gain of water from a shallow aquifer, if present) or lateral water movement, and because most runoff is prevented by the edge of the box, which is higher than the surrounding soil surface (fig. 1, right).

Weighing lysimeters are potentially the most accurate way to determine crop water use, and many different designs and weighing mechanisms have been used (Howell et al., 1991). The accuracy of any measurement system can be assessed as the root mean squared error of its calibration, typically determined by some form of least squares regression analysis. The resolution of a lysimeter system is different from, and often smaller than, the accuracy. Resolution in mm depth of water can be determined from the resolution of the datalogger, i.e., the smallest voltage difference that can be

determined by the datalogger (analog to digital conversion), multiplied by the lysimeter calibration slope. The theoretical lysimeter calibration slope (b , mm/mV/V) can be estimated in terms of mm depth of water per millivolts of load cell output per volt of load cell excitation:

$$b = \frac{L_c M_A}{O_r A_L} \quad (4)$$

where L_c is rated load cell capacity (kg), M_A is mechanical advantage (-), O_r is load cell rated output at full rated load (mV/V), and A_L is lysimeter surface area (m^2). Equation 4 assumes that the density of water is 1.000 Mg m^{-3} , so that 1 kg of mass change per square meter of lysimeter surface area is equivalent to 1 mm depth of water. In addition, load cell capacity is given in units of force, but for applications at the earth's surface, this may be converted usefully to units of mass, as used above. The local variation in the gravitational force and imperfections in lysimeter construction that affect the mechanical advantage are two reasons why lysimeter weighing systems must be calibrated rather than relying on equation 4 alone. From equation 4, it can be seen that lysimeter resolution can be increased by increasing the surface area (as in the case of the $>28 \text{ m}^2$ lysimeter of Pruitt and Angus, 1960), using a load cell with larger rated mV/V output at full load, using a load cell with smaller capacity, or designing to decrease the mechanical advantage of the weighing system. However, there are practical limits to all of these.

Direct-weighing lysimeters use load cells, often beam type or button type, to directly carry the total load of the lysimeter. The mechanical advantage is unity, but L_c is often very large. For example, the deck scale utilized by Schneider et al. (1998) at Bushland, Texas, had a load capacity of 13.6 Mg divided among four load beams, which summed together had a full-scale output of 1.5 mV/V, and the lysimeter surface area was 2.25 m^2 . The CR7X datalogger they used had a precision of $0.166 \mu\text{V}$. The theoretical calibration slope was 4032 mm/mV/V , and the actual calibration slope was 4159 mm/mV/V . The theoretical resolution was $0.000166 \text{ mV} \times 4032 \text{ mm/mV/V} = 0.67 \text{ mm}$, and the actual resolution was $0.000166 \text{ mV} \times 4159 \text{ mm/mV/V} = 0.69 \text{ mm}$, but the calibration accuracy (RMSE) was slightly better at 0.1 mm.

Balance beam weighing systems present some advantages for lysimeters because the resultant force can be counterbalanced easily so that a smaller load cell can be chosen to determine mass changes. For example, the 9 m^2 weighing

lysimeters at Bushland (Marek et al., 1988) used a balance beam counterweighted weighing system (model FS-7 agronomy scale, Cardinal Scale Manufacturing Co., Webb City, Mich.) with 100:1 mechanical advantage and a 22.68 kg load cell that had a full-scale output of ~ 3 mV/V. The theoretical calibration slope and resolution were 84 mm/mV/V and 0.014 mm, respectively. Calibration resulted in an accuracy of 0.045 mm (Howell et al., 1995) and an actual slope within 2% of the theoretical one. The disadvantage of this weighing system is the limited range possible before the counterweight must be adjusted to keep the load cell within range. For example, the Bushland lysimeters have a range of $\sim 3 \times 84 = \sim 252$ mm (depth of water equivalent) without counterweight adjustment. The Pullman soil at Bushland has field capacity and wilting point values of 0.33 and 0.18 m³ m⁻³, respectively, so that water uptake from field capacity to wilting point in a 1.5 m deep rooting zone would be $\sim 0.15 \times 1500 = 225$ mm. Thus, the lysimeter range is reasonable. In the 20 years since those lysimeters were installed, counterweight adjustment has been necessary up to twice per growing season in some years, but often not once in a growing season. Counterweight adjustment is more common for dryland crops that tend to dry the profile more than do irrigated ones. Fortunately, counterweight adjustment is simple and presents a nearly instantaneous scale output change that can be easily accommodated in data analysis for crop water use.

Due to the advantages and accuracy of weighing lysimeters, the MERIMIS team proposed to install a weighing lysimeter in the Jordan Valley. Since the design team leader possessed more than 20 years of experience in weighing lysimeter operation and design and nearly 30 years of experience with the neutron moisture meter (NMM), this decision was made with full understanding of the relative merits of weighing lysimeters versus the other major soil water balance method of determining crop water use using the NMM. The NMM requires careful soil-specific calibration, including calibration for depths near the surface and any horizons that may differ widely in texture or bulk density (Evet, 2008; Hignett and Evett, 2002). It also requires training for safety and proper use. In terms of experimental management and field plot design and maintenance, the NMM method is similar to weighing lysimetry in requiring experimental designs and management that minimize runoff and runoff, that feature uniform plant stands and heights over areas large enough to overcome fetch effects, that ensure uniform irrigation and fertilization, and that minimize effects due to experimenter entrances into the field. With regard to the latter, it is common that field entrances for weighing lysimeters are less frequent and less damaging to plants than those required for regular use of the NMM. This is not to say that the authors rejected the NMM, only to point out that it is not a simple, low-cost replacement for a weighing lysimeter. In fact, the MERIMIS team in Jordan and elsewhere employs the NMM in other irrigation experiments to determine crop water use and develop supporting data for the weighing lysimeter effort.

The MERIMIS partner at the National Center for Agricultural Research and Extension (NCARE) in Jordan agreed to host the lysimeter. The objectives of this article are to describe the planning, design, construction, calibration, and resulting capability of the lysimeter facility.

SITING AND DESIGN

SITING

Site selection for the lysimeter occurred in 2004 during visits by NCARE and USDA-ARS personnel to several locations. The Dayr Alla site (32° 11' 26" N, 35° 37' 06" E, 224 m below MSL) (fig. 2) was chosen for several reasons. Most irrigation in Jordan is in the valley, and the site is on a well established NCARE agricultural research station there. An agricultural micrometeorological weather station is located there as part of the MERIMIS weather network, and an eddy correlation system is sited 50 m to the west of the lysimeter site. A relatively large (100 × 200 m, 2 ha) field was available, providing adequate fetch in the prevailing E-W wind direction (up and down slope between the valley sides and the Jordan River). The Jordan Valley Authority main water distribution canal is adjacent to the station, and a reservoir and drip irrigation system exists to irrigate the field (water electrical conductivity is 0.75 to 1.5 dS m⁻¹). The location and soil are typical of irrigated areas in the Jordan Valley. The soil is deep and lacks both a shallow water table and strong horizonation. The site is approximately midway between the less saline irrigated areas to the north and the more saline irrigated areas to the south and is near the center of the most densely irrigated part of the valley (Development Area No. 23). Electrical power is available (convenient though not strictly required). Ongoing research and experienced personnel (both scientific and technical) bode well for continued scientific and technical support. A University of Jordan research farm is nearby, facilitating cooperative work and training of students.

DESIGN

The lysimeter design was similar to that of the large weighing lysimeters at the USDA-ARS laboratory at Bushland, Texas (Marek et al., 1988; Howell et al., 1995) with some important changes. It was found that surface dimensions of 2.4 × 3.0 m (vs. 3.0 × 3.0 m at Bushland) would accommodate the wide variety of plant row spacings used for different crops in the Jordan Valley, allowing row spacings that were integer divisors of 2.4 m when planted along the long axis of the lysimeter and row spacings that were integer divisors of 3.0 m when planted across the short axis of the lysimeter. A smaller surface area (e.g., 1.5 × 1.2 m) could have been chosen, but heat flux in the steel walls might have caused heating of the lysimeter soil compared with the field soil (Black et al., 1968; Dugas and Bland, 1991), and the smaller area would have decreased the resolution possible (eq. 4). A depth of 2.5 m was chosen to provide for a 2.4 m soil depth above the drainage filter bed. Van Bavel (1961) showed the necessity of depths >1.5 m in lysimeter design in order to avoid root zone soil profile water content differences between the field and lysimeter and to avoid preferential water uptake from the lysimeter bottom by deep-rooted plants. Since the lysimeter will provide basic ground truth for the MERIMIS irrigation scheduling system, it is likely that alfalfa will be grown at some point in order to determine alfalfa reference evapotranspiration in this environment. A deep lysimeter is required to accommodate this deep-rooted crop.

The field soil is composed of lake bed deposits that lack strong soil horizons, allowing use of a repacked soil tank rather than acquisition of a monolithic block of soil, which would have required lifting cranes of a capacity that was not avail-

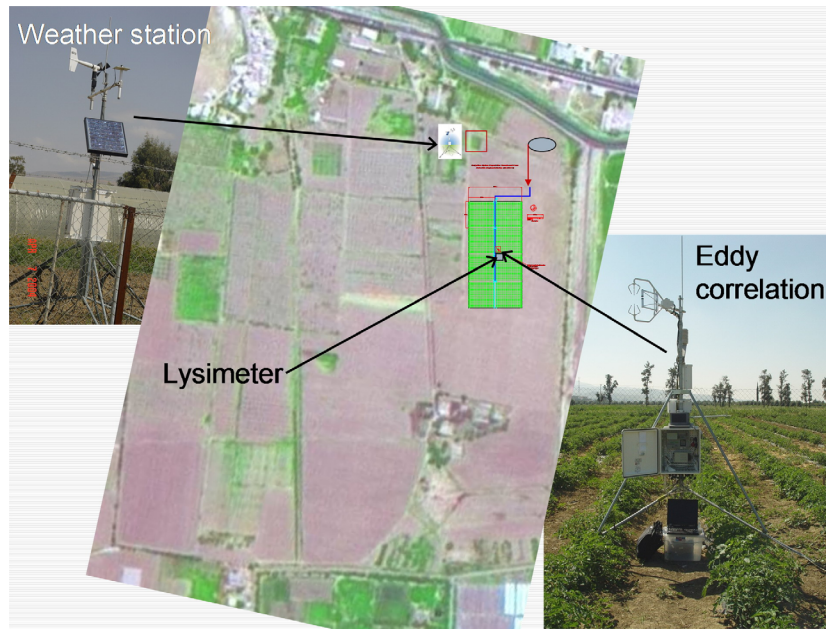


Figure 2. Satellite image of the Dayr Alla Agricultural Research Station showing the field where the lysimeter was installed (green rectangle), and photographs and locations of weather station and eddy correlation system.

able. The bulk density and texture are reasonably uniform to the 2.5 m depth. Thus, a repacked soil profile should provide for accurate crop water use measurements if bulk density is replicated during repacking and the soil is repacked in layers corresponding to the original soil profile (Pruitt and Angus, 1960; van Bavel and Myers, 1962). A deeper floor for the outer enclosure was designed so that the roof could be at least 1.5 m below the soil surface (vs. 0.5 to 0.8 m at Bushland), allowing a reservoir of soil water and providing for even crop growth over the roofed area, field, and lysimeter without supplemental irrigation. The design included a ship-type access ladder to ease entry into and egress from the lysimeter. The access door was placed 2 m farther from the lysimeter surface (~3.5 m vs. the ~1.5 m at Bushland) to minimize disturbance of the crop near the lysimeter when entering and exiting the lysimeter. Similar to the Bushland lysimeters, electrical power (240 VAC, 50 Hz) was provided by cable buried at 1 m depth in 50 mm rigid polyvinyl chloride (PVC) electrical conduit.

The scale was a double wishbone, lever arm type with a transverse lever assembly transferring the load from both wishbones to the final, counterbalanced lever and load cell assembly (model FS-9, Cardinal Scale Manufacturing Co., Webb City, Mo.). This scale had a mechanical advantage of 1000 as shipped, which was too large to give the desired resolution when coupled with the chosen datalogger. Rather than purchase a much more expensive datalogger with greater resolution, the balance's final lever arm was shortened to obtain an overall mechanical advantage of approximately 300. With appropriate counterbalancing mass, the 4.54 kg (10 lb) load cell (model SM-10, Interface, Tucson, Arizona; www.interfaceforce.com) had sufficient range to encompass mass changes that typically occur over a single cropping season. A set of small counterbalance masses allowed fine tuning of the range and allowed compensation for larger lysimeter mass changes that might occur over longer periods or due to particular experimental protocols (for example, heavy versus light irrigation). The load cell was sensed using a four-wire bridge

circuit connected to a datalogger (model CR3000, Campbell Scientific, Inc., Logan, Utah) with 0.67 μV resolution. A six-wire bridge was not used because temperature changes inside the lysimeter enclosure are minimal and slow. Given a mechanical advantage of ~300, load cell rated output of 3 mV/V, and lysimeter surface area of 7.2 m^2 , an estimated calibration slope of 61 mm/mV/V and estimated resolution of 0.04 mm were calculated using equation 4.

The datalogger was used to sense other instruments employed for environmental monitoring. Data were stored in a compact flash card using a datalogger accessory module (model CFM100 CompactFlash module, Campbell Scientific, Inc., Logan, Utah). Environmental conditions are determined using sensors as listed in table 1. Additional sensors may be added in the future for specific experiments (e.g., soil heat flux, soil temperature, soil moisture, etc.). Using multiplexers, the chosen datalogger should be sufficient for most foreseeable additional sensors.

The weighing lysimeter consists of a 2.4 \times 3 m surface area soil tank (2.5 m deep) that rests on the scale within an underground enclosure such that the top of the soil tank is

Table 1. Sensors employed to determine environmental conditions.

Condition	Unit	Sensor (Model)
Wind speed	m s^{-1}	Sonic anemometer (WindSonic-L)
Solar radiation	W m^{-2}	Silicon pyranometer (LI200X-L Li-Cor)
Air temperature and relative humidity	$^{\circ}\text{C}$ and %	Temperature and RH probe (HMP45C-L-GM) with gill radiation shield (41003-5)
Barometric pressure	Pa	Barometric pressure (CS100 Setra 278)
Net radiation	W m^{-2}	Net radiometer (NR-Lite-L, Kipp and Zonen)
Precipitation	mm	Tipping-bucket rain gauge with 0.1 mm per tip (TE525MM-L, 24.5 cm)

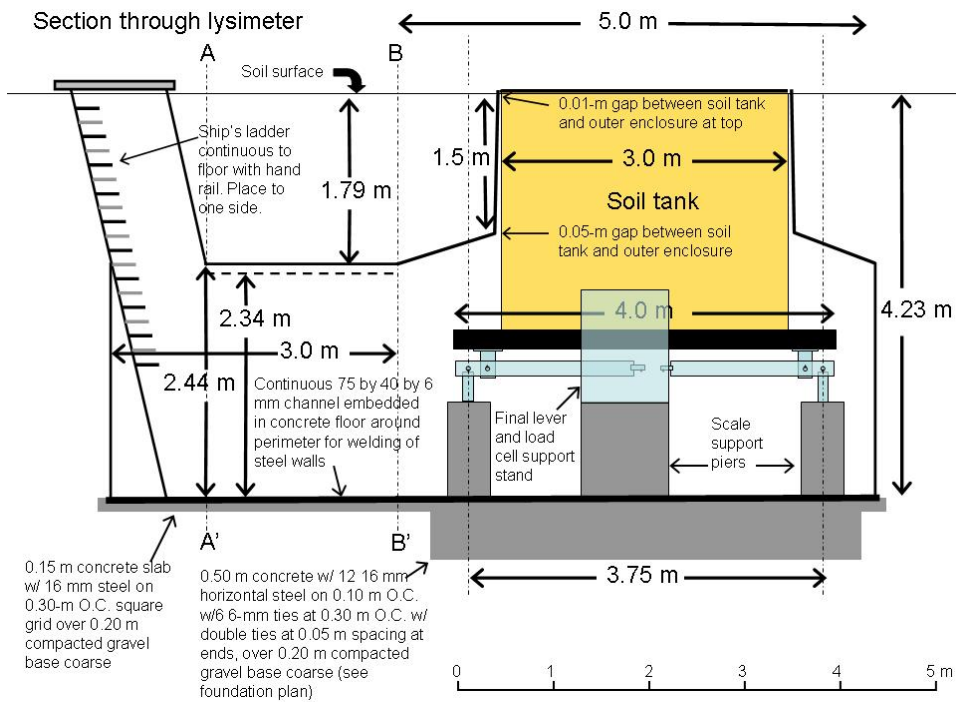


Figure 3. Cross-section through lysimeter showing soil tank, outer enclosure, access way to entrance tunnel, and hatch. Not all items shown are in the same plane. The foundation and slab, steel channel in slab, scale support piers, scale, final lever and load cell support stand, main girder, and soil tank are not in the plane of the cross-section but are shown for completeness. Roof support columns and horizontal and vertical reinforcing I-beams are not shown. The scale mechanism is shown in blue, the soil tank in yellow.

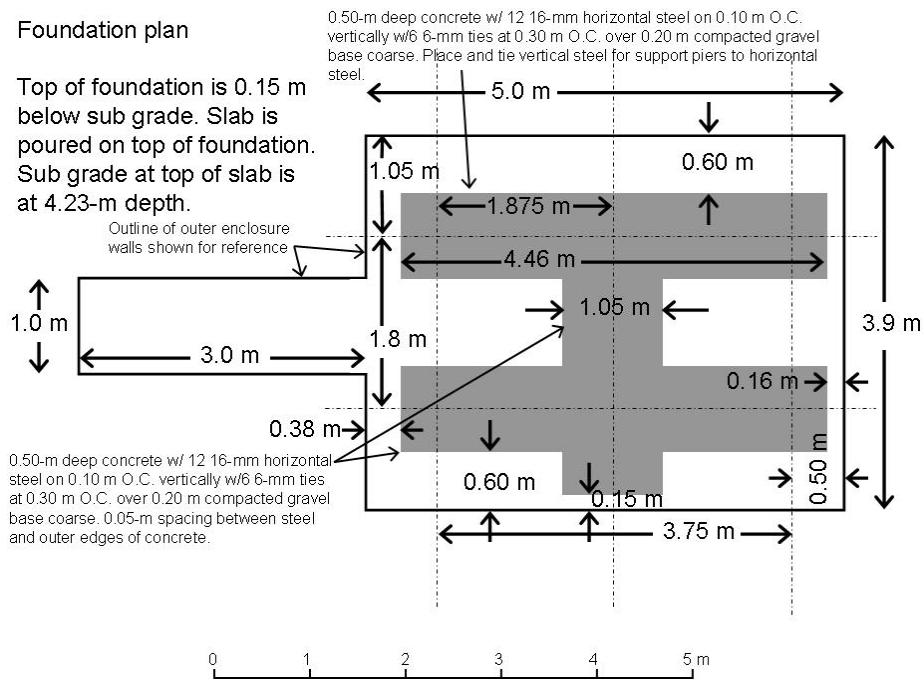


Figure 4. Foundation plan.

0.05 m above the field soil surface and the soil in the tank is at the same elevation as that in the adjacent field (fig. 3). The scale, which is 0.48 m tall, rests on six 1 m tall reinforced concrete piers, which in turn rest on a 0.15 m thick reinforced concrete slab supported by a 0.50 m thick reinforced concrete foundation under the slab (fig. 4). The outer enclosure was welded of 10 mm sheet steel and reinforced with 0.10 m I-beams. A continuous 75 × 40 mm steel channel was em-

bedded in the periphery of the concrete slab such that the top was at slab grade, and the channel was welded to the slab reinforcing steel. The outer enclosure walls were continuously welded to this steel channel. Steel was chosen for the outer enclosure walls and roof to prevent water transmission to the inside under irrigated conditions. The concrete slab and foundation rest on 0.20 m of compacted crushed stone to prevent water transmission upward to and through the slab.

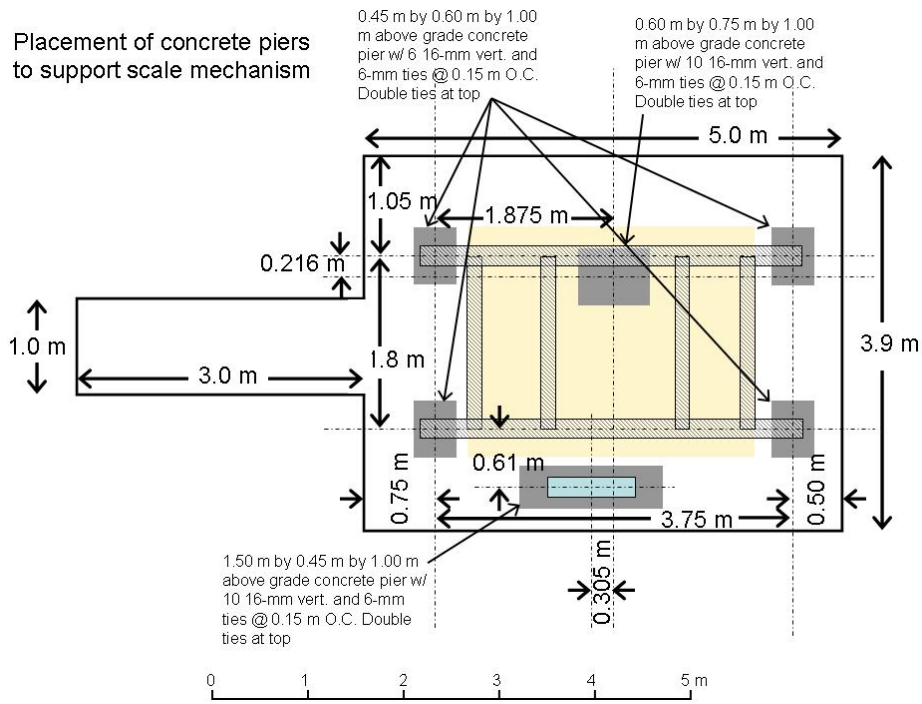


Figure 5. Placement of reinforced concrete scale support piers.

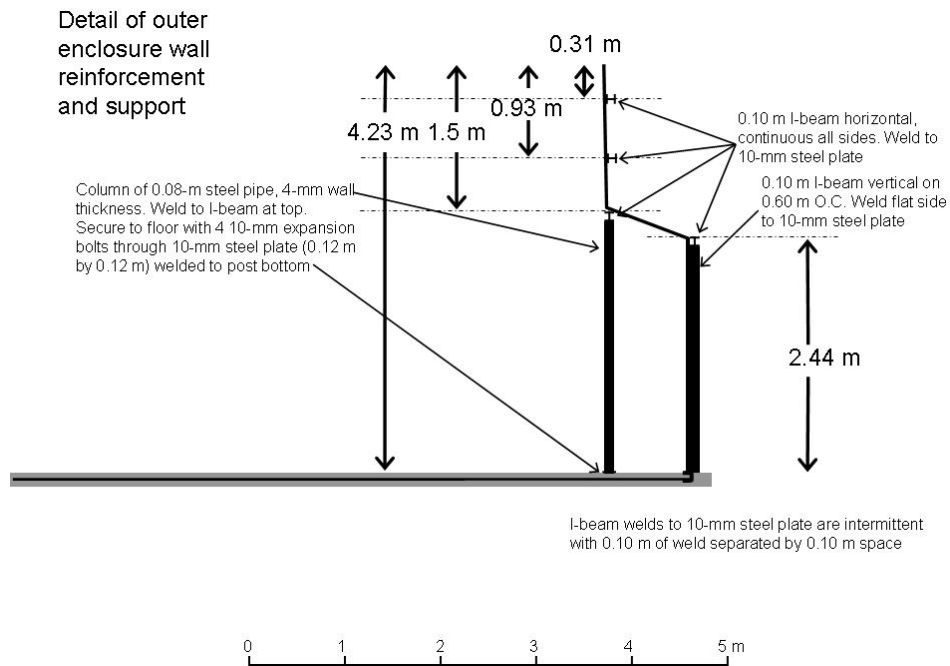


Figure 6. Detail of outer enclosure and roof reinforcement and support.

At floor grade, the plan is a 5.0×3.9 m rectangle with a 1.0×3.0 m access tunnel connected to one short side of the rectangle (figs. 4 and 5). The larger rectangle houses the scale. The outer enclosure consisted of two sets of walls. The upper enclosure walls surround the upper part of the soil tank (fig. 1) and were set at an angle so as to be separated from the soil tank by 0.05 m at the bottom of the wall and 0.01 m at the top of the wall. The two sets of walls were joined by a slanted roof (figs. 1 and 6).

CONSTRUCTION

EXCAVATION FOR SLAB AND FOUNDATION

The concrete slab served as the enclosure's floor, the top of which was at 4.23 m below grade. The excavation was 4.58 m deep to accommodate the depth of the compacted gravel and slab, except where the foundation placement required trenching to 5.08 m depth. The slab was 5.2×4.1 m in the main part, with a 1.2×3 m extension in the center of the short east side where the access tunnel was built (fig. 4). Excavation sides were stepped to a 1:2 grade to prevent col-

lapse. Excavation proceeded in 50 cm deep layers, with each successive layer placed in a separate pile and identified with a weather-proof placard. Excavation in 0.50 m layers was necessary to preserve, to the extent possible, the natural soil layering in the completed lysimeter installation (both in the soil tank and in re-packing soil around the outer enclosure). The total excavated soil volume was approximately 330 m³.

FOUNDATION, SLAB, AND SUPPORT PIER CONSTRUCTION

In the 0.50 m thick foundation, twelve 16 mm diameter horizontal steel rods were placed on 0.10 m center-to-center (O.C.) vertical spacing and on 0.35 m horizontal spacing. Rods were tied with 6 mm diameter stirrups at 30 cm spacing with double stirrups at the ends. At least 0.05 m spacing was maintained between the steel and the outer edges of the concrete. Vertical steel rods for the scale support piers were placed according to figure 5 and tied to the foundation steel. The slab was formed to an elevation 4.23 m below grade. Reinforcing steel of 16 mm diameter was placed at 30 cm O.C. in both directions and centered in the 0.15 m thick slab using 0.07 m tall concrete block pieces and rocks. An 80 × 40 × 6 mm steel C-channel was placed to be flush with the top of the finished slab and to be centered under the outer enclosure steel wall (fig. 4). Steel channel was welded at corners and all joints. Steel channel was centered on the enclosure wall outline so that the enclosure walls could be welded to the center of the top flange of the channel. A 0.30 m diameter × 0.30 m deep sump was formed in one corner of the slab for collection of any water that inadvertently enters the enclosure. The concrete contained 4 parts by mass of sharp washed silica sand, 8 parts by mass of washed gravel, and 3.5 parts by mass of Portland cement (class 250/315) and was mixed with clean, non-saline water to obtain no more than a 0.10 m slump (using a 0.30 m cone mold). The slab and foundation were poured together, and the slab was troweled smooth. The slab was covered with sand after finishing, and the sand was wetted twice daily for seven days to cure the slab.

Reinforcing steel for the scale support piers was tied to vertical steel that was tied to the foundation steel. Forms for the piers were constructed of 6 mm sheet steel, placed as shown in figure 5, and the form tops were leveled to an elevation of 3.23 m below grade. Concrete piers were poured using the same mix as for the foundation. Piers were screeded flush with the form tops, and anchor bolts were placed in position to accommodate the scale main lever stands, transverse lever stand, and counterbalance/load cell fulcrum stand.

LOWER ENCLOSURE WALL CONSTRUCTION AND SCALE INSTALLATION

The lower enclosure walls are vertical and were attached to the slab at floor grade by continuous welding to the steel channel embedded in the slab. Vertical 0.10 m steel I-beams spaced 0.60 m O.C. were welded to the outside of the steel walls and to a continuous I-beam collar set flush with the top of the 2.44 m tall vertical walls (fig. 6). The tunnel was similarly reinforced on the outside vertical surfaces. At the distal end of the tunnel, an access way with ship-type ladder and hatch was built to allow access from the surface to the tunnel (fig. 2). The access way to the tunnel was not reinforced from the elevation of the tunnel roof to the access hatch. The tunnel roof was 10 mm steel sheet supported at an angle from horizontal by the walls of the tunnel, one of which was 0.10 m

taller than the other. The angle was necessary to drain water from the top of the roof. A 0.1 × 1.0 m piece of 10 mm steel sheet was welded to each end of the tunnel to close off the gap between the tunnel roof and other roof components. The scale was installed per factory instructions except that the main load support girders were re-arranged by moving the outside two cross-girders inward by 0.50 m so that they would be directly underneath the soil tank.

SOIL TANK CONSTRUCTION AND PLACEMENT

The soil tank was constructed of 10 mm mild steel sheet with internal reinforcement (fig. 7). Sheets were joined with continuous butt welds to produce a watertight tank. Wall distortion from a right rectangular shape was prevented with 0.10 m steel angle reinforcement placed horizontally and welded intermittently in 0.10 m swaths to the interior walls at 0.50 m vertical spacing. To further prevent wall distortion, two 16 mm diameter tie rods were welded to the centers of opposite side walls and to the steel angle reinforcement at 0.50 m below the top of the tank. The tank was placed on the scale girders, centered end to end and side to side, with the long axis of the tank coincident with the long axis of the scale girders. On the outsides of the main girders, the tank overlapped the main girders by 0.20 m on the short axis, since the spacing of the main girders was 2.0 m outside to outside and the tank width was 2.4 m. The inside of the soil tank was painted with two coats of white epoxy enamel over a primer coat.

UPPER ENCLOSURE WALL AND ROOF CONSTRUCTION

Roof support columns were placed and bolted to the floor slab with expansion bolts (fig. 8), and a continuous 0.10 m steel I-beam was welded to the top of the support posts on all sides with welded joints at the corners. Spacing between the I-beam and soil tank was designed to be 0.05 m on all sides. The upper part of the upper enclosure was pre-made and lowered onto the supporting I-beam, adjusted slightly to be equidistant from the soil tank at the top, and then welded in place. The enclosure roof was constructed of 10 mm sheet steel spanning the gap between the horizontal I-beam collar on top of the support posts and the horizontal I-beam collar at the top of the lower enclosure wall reinforcement (fig. 7). All seams were continuously welded.

ACCESS LADDER AND ENTRY SHAFT

The access shaft was constructed of 10 mm steel plate placed at a 75° angle upwards from the horizontal, beginning at the top of the distal end of the entry tunnel (figs. 1 and 9). It was 1 m (same width as tunnel) × ~1.15 m (1.05 m perpendicular to the shaft wall) in the horizontal plane. The ladder was a ship-type, with self-cleaning, non-slip treads welded at 30 cm vertical spacing to 5 × 15 cm steel channel risers positioned 10 cm away from the shaft wall. At the top end of the ladder, short sections of 5 × 15 cm steel channel were placed horizontally and welded to the risers and to the wall to terminate the ladder and provide support for a non-slip, self-cleaning platform. Ladder rails on each side were fabricated of 40 mm steel tubing. The ladder, which is 0.60 m wide, was placed as far as possible to one side of the shaft so as to allow the lowering of items by rope from the hatch to the floor of the enclosure. The roof hatch was a Bilco type E aluminum hatch, which required a 0.914 × 0.914 m frame opening. At

Detail of soil tank

Soil tank inside dimensions: 3 m by 2.4 m by 2.5 m deep

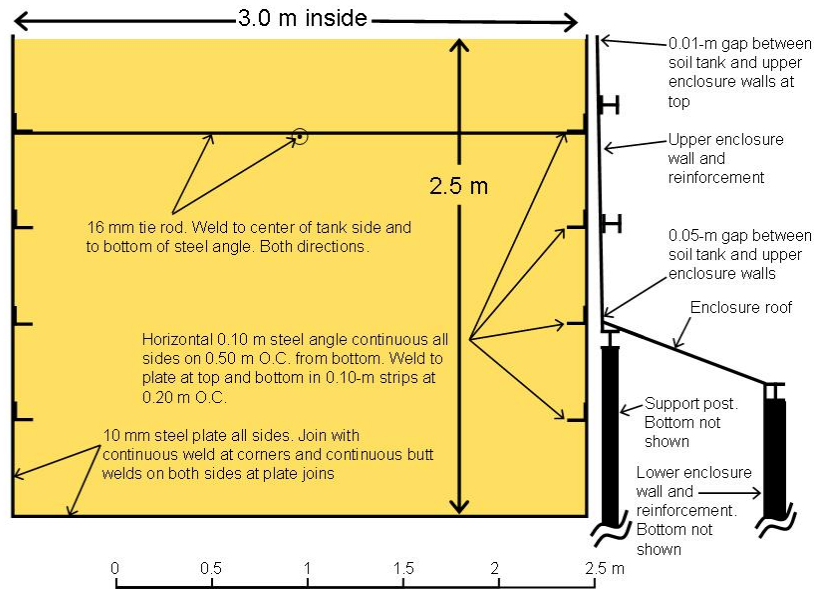


Figure 7. Soil tank construction showing internal reinforcement with steel angle and tie rods. Also shown is one side of outer enclosure upper and lower walls, roof, and reinforcement.

Placement of columns for roof support.

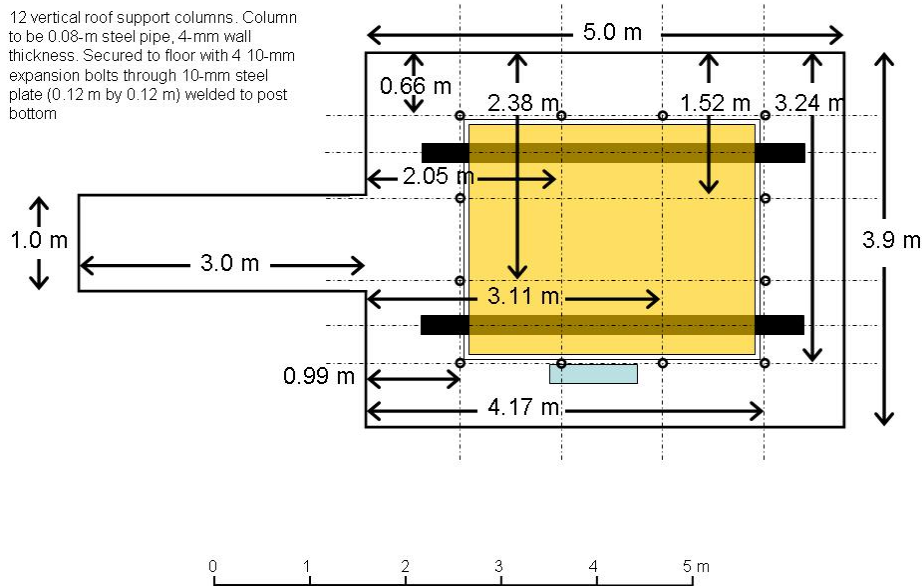


Figure 8. Placement of roof support columns.

0.05 m above grade, the top of the access shaft was framed to create a curb of this size using 10 mm steel sheet to provide a 0.12 m tall vertical steel curb with outside dimensions of 0.914 × 0.914 m (fig. 9, bottom).

COATINGS

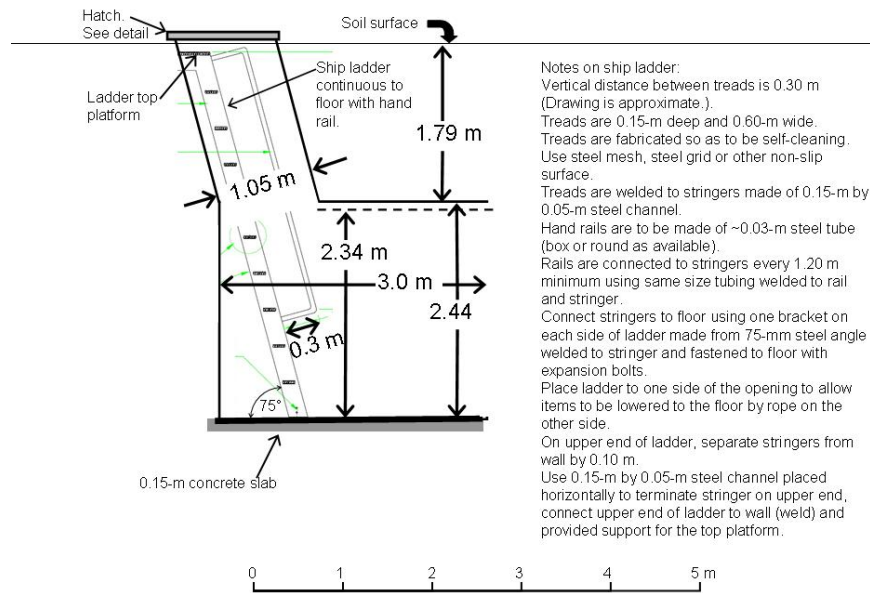
The outside surfaces of the outer enclosure, access tunnel, and entry shaft were primed and painted, and then coated with tar, burlap, and a second coat of tar to prevent water penetration to the steel and resulting rust. The interior surfaces of access shaft, tunnel and outer enclosure, and the exterior

surface of the soil box were primed and painted with light gray enamel.

DRAINAGE SYSTEM AND SOIL PACKING

The drainage system inside the soil box consisted of 16 fritted stainless steel filter tubes (type 316L sintered, porous stainless steel filter tubes, 3.8 cm diameter and 76 cm long, Mott Metallurgical Corporation, Farmington, Conn.; bubbling pressure = 10 kPa, particle size rating = 0.5 micron) placed as shown in figure 10 and plumbed to the outside using 1/4-inch diameter stainless steel tubing and compression fit-

Section through entry and access tunnel



Detail of Hatch Curb

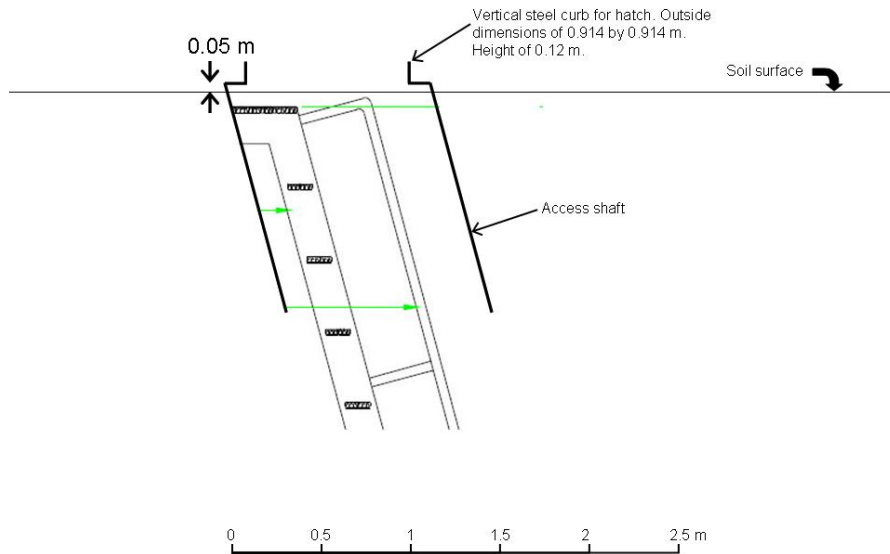


Figure 9. (top) Section through entry showing access hatch, shaft, ladder, and tunnel, and (bottom) section through detail of curb for entry hatch.

tings. Soil tank wall penetrations were made using stainless steel couplers (1/4-inch NPT) welded into holes drilled at 0.05 m from the tank bottom (welded on both sides). Filter tubes were embedded in a 0.10 m thick layer of fine silica sand. After drainage system installation, dry, crushed, and sieved soil was placed in the tank in 0.10 m layers and compacted by hand. Soil was placed by layer in the reverse order of its removal from the excavation. Soil was packed around the outer enclosure in the same manner and finished to match the elevation of the surrounding field. The gap between the soil box and outer enclosure was covered using a 0.64 mm (0.025 in.) EPDM nylon fabric glued to the inside of the soil box and outside of the outer enclosure with rubber cement such that the fabric was loose enough to avoid causing tension forces on the soil box.

Outside the soil box, high-density polyethylene plastic nipples were screwed into the 1/4-inch NPT couplers to provide a barbed nipple for connection to 1/4-inch PVC vinyl vacuum tubing, which was used to connect the flow from the eight filters that were placed in the center of the soil tank into one tube that led to one drainage collection tank and which likewise was used to collect the flow from the eight filters placed around the periphery of the soil tank into a second drainage tank. Each tank was suspended from the soil tank support girders by a 114 kg (250 lb) load cell so that flow into the tank would not change the mass of the lysimeter and so that the drainage rate could be recorded by measuring the mass of the drainage water with the datalogger. Drainage tanks were made from epoxy resin fiberglass sand filter casings fitted with a rigid PVC closure in which 1/4-inch barbed nipples were plumbed for collection of drainage and for ap-

Detail of drainage system

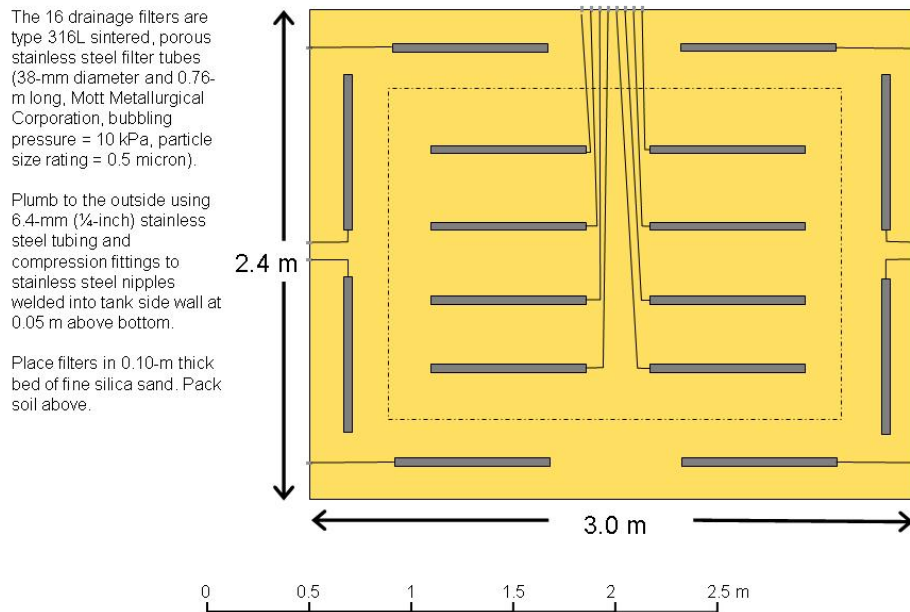


Figure 10. Placement of drainage filters at bottom of soil tank and plumbing to outside of tank.

plication of vacuum from a pump. The vacuum pump was controlled by a continuous use rated industrial differential vacuum switch (type GAQ-21, class 9016, series C, Square D Company, Raleigh, N.C.) set to turn on the pump when vacuum declined to 9 kPa of suction and to turn off the pump when vacuum increased to 11 kPa of suction. It was protected with a fuse on the powered side of the circuit.

ELECTRICAL

Electrical power (240 VAC, 50 Hz) was supplied by a cable buried at 1 m depth in a 50 mm diameter rigid PVC conduit connected to a watertight fitting through the side of the access tunnel to a main switch and breaker (fuse) box at 1.5 m height above the floor in the entrance tunnel. Power was distributed from the breaker box to electrical outlets and fluorescent lights through electrical conduit and approved fixtures affixed to the enclosure walls and roof. A light switch was placed on the entry tunnel wall near the ladder.

CALIBRATION AND TESTING

The lysimeter calibration slope (b) was estimated from equation 4 to be 61 mm/mV/V. Since the resolution of the CR3000 datalogger is 0.67 μ V, the theoretical resolution was 0.04 mm. However, resolution is not the same as accuracy of measurement, which can only be determined by calibration of the measurement system. The root mean squared error (RMSE) of the calibration least squares regression is the statistic used in science and engineering to establish measurement system accuracy. Since the measurement system output is expected to be linear with mass changes, we used a linear least squares regression of mass (in equivalent mm of water depth) versus load cell output determined by the datalogger.

The minimal range of mass used in the calibration was determined from the expected maximal mass change during an

irrigation season with the assumption that management would not allow the soil in the root zone to dry by more than 50% of available water holding capacity. Field capacity and permanent wilting point of the soil are 0.33 and 0.18 $\text{m}^3 \text{m}^{-3}$, respectively, so that 50% of AWHC is 0.075 $\text{m}^3 \text{m}^{-3}$. The deepest active rooting zone was estimated to be 1.5 m, so that the mass of water change was calculated as $0.075 \times 7.2 \times 1.5 \times 1000 \text{ kg m}^{-3} = 799 \text{ kg}$. Calibration was done with the lysimeter soil surface covered by plastic sheeting to prevent evaporative losses. The datalogger was programmed for a four-wire bridge with 950 mV/V excitation and input range of 1000 mV/V for the voltage drop across the full bridge and 50 mV/V for the bridge output voltage. Readings were taken at 1 Hz with mean and standard deviation values reported at 1 min intervals. Initial load cell readings were taken for 10 min. Masses were then added in approximately 50 kg increments every 10 min until approximately 700 kg were loaded onto the lysimeter. After a 10 min wait, the masses were unloaded in approximately 50 kg increments every 10 min. After all loaded mass was removed, load cell measurements were continued for 10 min. Data were screened to remove data recorded during placement or removal of masses, and the remaining data were processed by linear least squares regression in three ways: data for mass loading only, data for mass unloading only, and all data. The lysimeter was tested by observing mass change for 24 h with the lysimeter covered with plastic to prevent evaporative losses.

Testing continued during the first season of operation, which began with the installation of a surface drip irrigation system followed by the planting of sweet corn (*Zea mays* L., variety Merit) on 22 June 2008. Drip tubing (18 mm diameter, type GR, Mais Irrigation Company, Amman, Jordan) was installed on a 1.5 m spacing in both the field and lysimeter, but the two drip tubes in the field that were lined up on the lysimeter were routed around the lysimeter using polyethylene hose and were continued in a straight line in the field on



Figure 11. Surface drip irrigation system installed in field and on weighing lysimeter.

the other side (fig. 11). A separate metered hose led to the lysimeter, where it was connected to two drip tubes placed on the lysimeter in line with those in the field. Emitters were an in-line long path type, were spaced at 0.40 m, and had a flow rate of 3.87 L h⁻¹ at nominal operating pressure of 200 kPa.

RESULTS AND DISCUSSION

The calibration equation from linear regression was:

$$S = -59.89 + 64.437(x) \quad (5)$$

where S is water storage (mm), and x is the load cell reading from the datalogger (mV/V) (fig. 12). The RMSE was 0.109 mm, and r^2 was 0.9999. Resolution of the datalogger output was 0.001 mV/V, resulting in a 0.064 mm resolution for the lysimeter. Thus, the calibration slope and actual data resolution closely matched the predicted values.

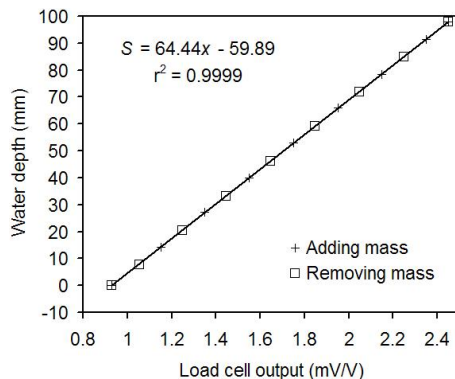


Figure 12. Lysimeter calibration results, where S is soil water storage (mm) and x is output of the load cell (mV/V). The intercept term (-59.89) is arbitrary.

INSTALLATION CHALLENGES AND DESIGN COMPARISONS

Lysimeter construction began in autumn 2006, and installation was completed in May 2008. The main challenge was lengthy waits between phases of construction that were caused variously by contracting problems, equipment lost in shipping from the U.S., and delays for funding renewals. These problems are not unique to Jordan. Indeed, many lysimeter installations suffer similar problems and similar start to finish construction times. The major steel constructs were completed in a machine shop in Amman and trucked to the site on a flatbed trailer. Local welding, electrical, and construction labor was used to complete the facility.

The lysimeter design had the important advantages of easy access to the weighing mechanism and a weighing mechanism that can be entirely refurbished and put in like-new condition at any time without removing the soil container. This avoids the costly and time-consuming (sometimes months) repairs that are necessary when weighing systems fail and access to the scale and soil box from below ground is not provided (e.g., Marek et al., 2006; Schneider et al., 1998). A lower-cost, direct-weighing lysimeter built with no access below the surface at Bushland, Texas (Howell et al., 2000) experienced a weighing system failure due to lightning that required removal of the soil container and scale, which took many weeks, was costly, and disrupted an entire measurement season. A scale failure in a similar lysimeter at Uvalde, Texas, caused Marek et al. (2006) to point out that this “closed” type of design has the potential to result in costly repairs and lengthy loss of data when scales fail.

The design differed from that of other lysimeters in the region in important ways. The two direct-weighing lysimeters at Ismailia, Egypt, described by Schneider et al. (1998) were of the “closed” type and so cannot be easily repaired. They were only 1.5 m deep and 3 m² in surface area and had gravity drainage to a slotted plastic pipe. The two direct-weighing

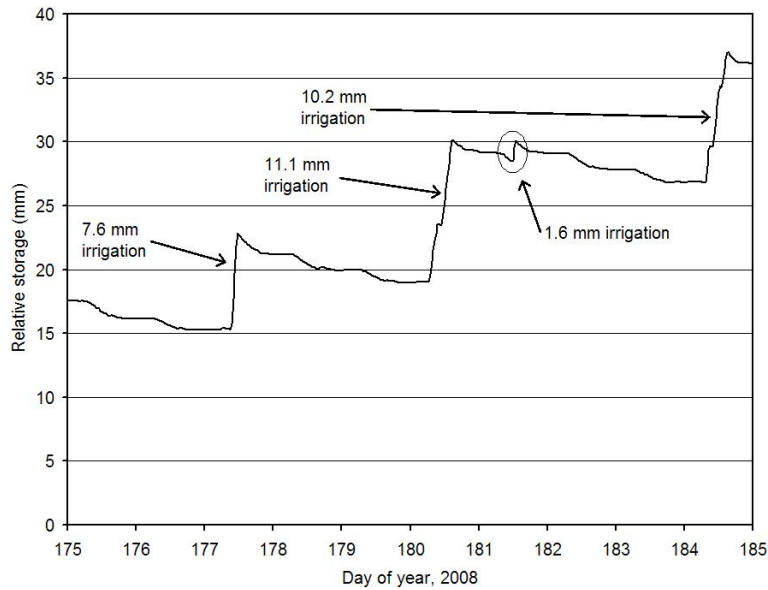


Figure 13. Lysimeter response to five irrigation events early in the season in terms of the relative storage in mm of water. Storage decreased during the day and remained relatively static at night.

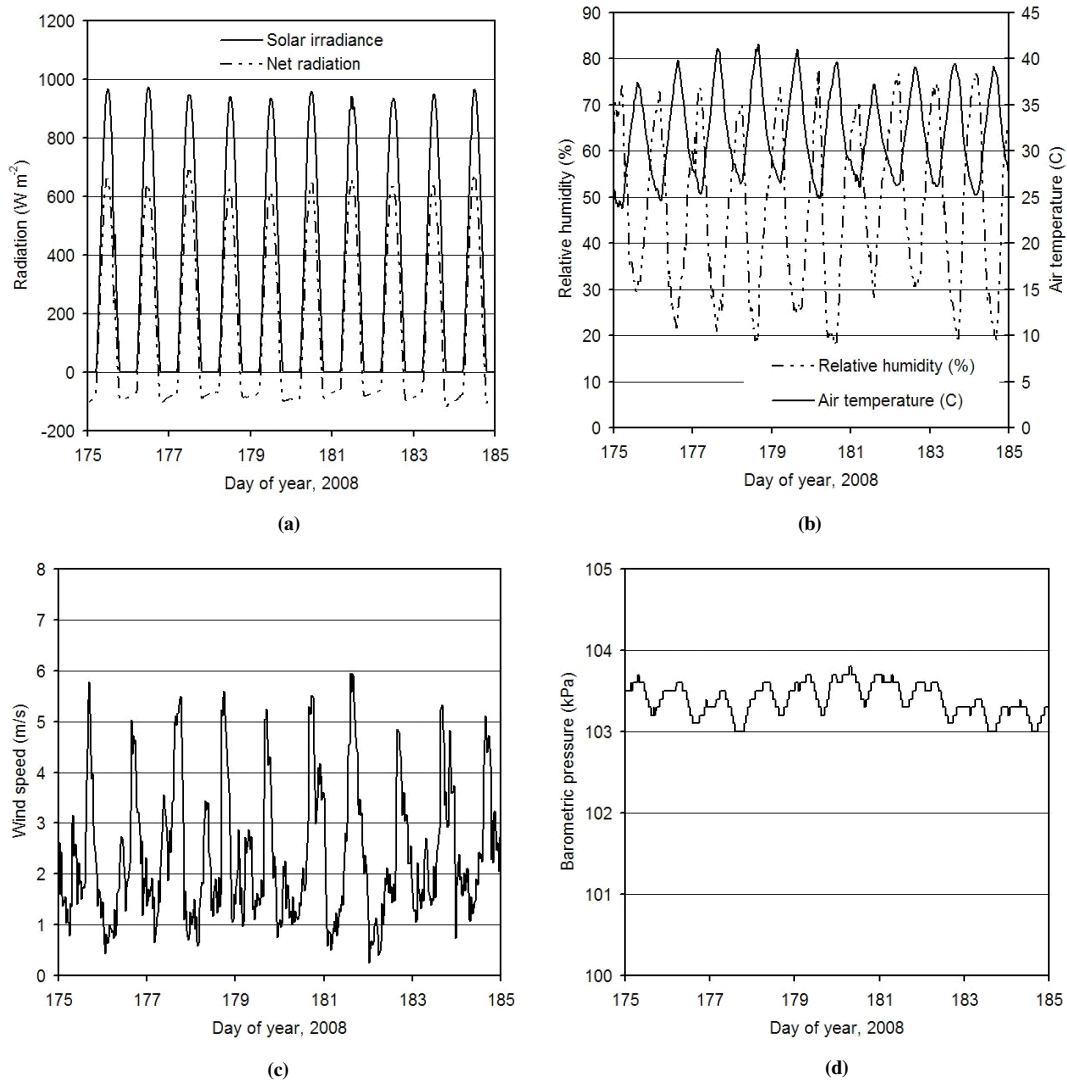


Figure 14. Example of meteorological data measured at 2 m height at the lysimeter for days of year 175 to 185 (23 June to 4 July 2008): (a) solar irradiance and net radiation, (b) air temperature and relative humidity, (c) wind speed, and (d) barometric pressure.

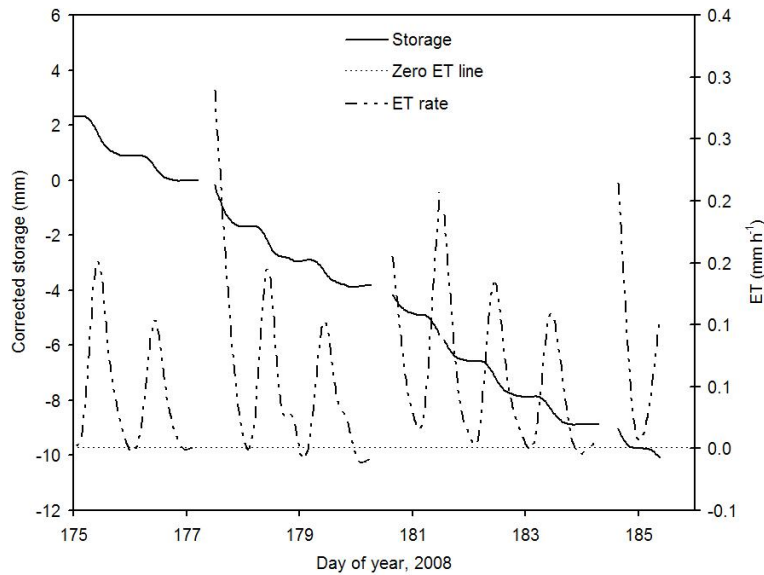


Figure 15. Example of relative storage corrected for irrigation amounts and evapotranspiration (ET) rate calculated as the first derivative of storage over four irrigation cycles. Irrigation occurred on DOY 174, 177, 180, and 184.

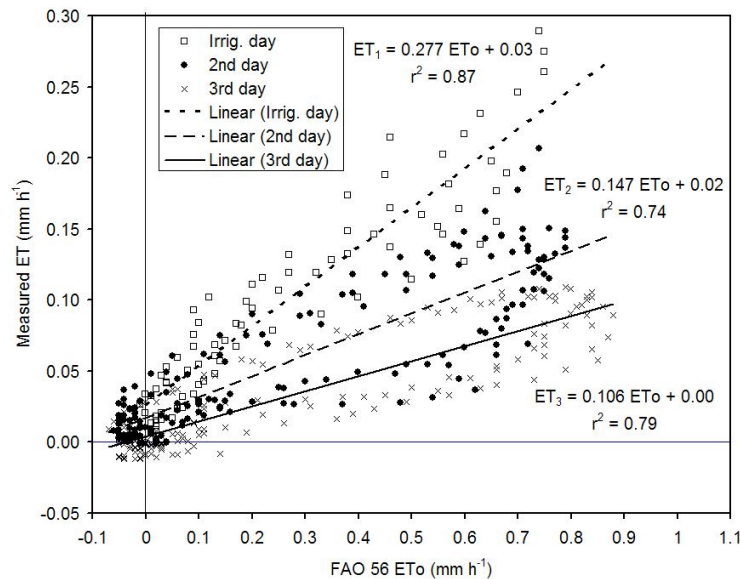


Figure 16. Evapotranspiration (ET) rate on the day of irrigation (after irrigation), on the day after irrigation (second day), and on the third day compared with grass reference evapotranspiration (ETo) calculated according to FAO 56 (Allen et al., 1998). Data are for four irrigation cycles. Irrigation occurred on DOY 174, 177, 180, and 184.

lysimeters at Kerman, Iran, were circular (Barani and Khanjani, 2002), which makes it difficult to ensure that leaf area is evenly distributed inside and outside of the lysimeters. They were 1.75 m deep, had a surface area of 7.07 m², and had gravity drainage through a bed of porous volcanic gravel. Their measurement error was 0.14 mm. Access was provided via an underground room, but the soil thickness above the roof of the underground room was only 0.5 m, not enough to avoid plant-available water supply problems to a growing crop in an arid region unless irrigated frequently.

EXAMPLE CROP WATER USE AND WEATHER DATA

The crop reached the 4 to 5 leaf stage on 1 July 2008. Example data from 24 June to 4 July 2008, day of year (DOY) 175 to 185, show the lysimeter response to four irrigation

events and intervening periods of evaporative loss in terms of the relative lysimeter storage in mm of water (fig. 13). As expected, rapid losses of mass to evaporation during the day led to decreases in storage; at night, the storage values were static. Because the soil profile was relatively dry at this point, irrigations were aimed at increasing the water content in the upper profile.

Example weather data for the same period show that skies were clear, with solar irradiance peaking at values between 900 and 1000 W m⁻² and net radiation values peaking at values between 600 and 700 W m⁻² (fig. 14a). These values are appropriate for a site at 224 m below sea level. Even though the site is in a desert environment, relative humidity values cycled between 50% and 80% during most 24 h periods, with relative humidity being largest at night when temperatures

**Table 2. Costs for weighing lysimeter construction in the Jordan Valley, Jordan.
Costs in Jordanian dinars (JD) calculated at 0.708 JD per U.S. dollar.**

No.	Item	Cost, Jordanian Dinar (JD)	Cost, U.S. Dollar (\$)
1	Shipping (U.S. to site)	5,494.40	\$7,760.45
2	Excavation (machinery and labor).	1867.17	\$2,637.25
3	Concrete construction and labor.	5123.74	\$7,236.921
4	Steel construction (soil tank, outside enclosure, stairs, painting, etc.)	12735.60	\$17,988.14
5	Local transportation and travel costs for personnel	787.00	\$1,111.58
6	Equipment transportation, clearance stamps and other fees (from the airport to the site)	710.80	\$1,003.96
7	Electrical equipments and power supply parts	554.51	\$783.21
8	Miscellaneous (small parts, connections, fittings, small equipment, and items purchased separately with an item value of less than 50 JD)	1703.84	\$2,406.55
9	Drainage system (filter tubes, tubing, connectors, vacuum pump, and tanks)	4,228.51	\$5,972.47
10	Lysimeter scale	5,310.00	\$7,500.00
11	Load cells, clevises and rod end bearings	478.57	\$675.95
12	Roof hatch, aluminum	604.99	\$854.50
13	EPDM coated nylon fabric	260.95	\$368.57
14	Eight turnbuckles	383.74	\$542.00
15	Datalogger and weather sensors in table 1	6,068.15	\$8,570.83
Total cost		46,311.97 JD	\$65,412.38

were smallest (as small as 24°C) (fig. 14b). Daytime temperatures ranged up to 42°C. The pronounced daily cycles of solar irradiance, temperature, and humidity occurred in concert with daily cycles of wind speed, which peaked at approximately 1700 h each day, and barometric pressure, which peaked at approximately 0800 h each day, shortly after air temperatures reached their minimum at approximately 0500 h. Daily cycles of wind speed are not unexpected in a long, deep valley such as the Jordan River Valley (JRV). Indeed, Alpert and Getenio (1988) modeled such patterns in the JRV using a three-dimensional mesoscale model.

Storage data were corrected for irrigation amounts, and the first derivative was taken using 21/15 Savitsky-Golay data/derivative smoothing (Gorry, 1990; Savitsky and Golay, 1964) to calculate the ET rate (fig. 15). Note that since the starting value of storage was arbitrary, negative values of storage may result from correction for irrigation. The ET rates showed nearly sinusoidal variations similar to those evident in the solar irradiance data (fig. 14a) except for late afternoon rate changes on DOY 178 and 179 that were associated with abrupt declines in wind speed. The ET rates were greatest immediately after irrigations and declined on subsequent days. Comparison with grass reference evapotranspiration (ET_o) calculated using the FAO 56 equations (Allen et al., 1998) showed that ET over four irrigation cycles was 0.28 of ET_o immediately after drip irrigation, 0.15 of ET_o on the second day, and 0.11 of ET_o on the third day (fig. 16). These relatively low rates would be expected given the early crop growth stage and the wide (1.5 m) drip tape spacing that resulted in incomplete surface wetting during irrigation. Hysteretic behavior of the data, which is particularly obvious at the smaller ET rates, is probably due to nighttime rewetting of the soil surface from below coupled with the rapid reduction of soil hydraulic conductivity as the soil dries, which would lead to more rapid ET rates early in the day followed by a decline of ET rate later in the day.

SUMMARY

The total expenditure, exclusive of travel costs for USDA-ARS personnel, was \$65,000.00 U.S., including the weather

sensors (table 2). This is very reasonable for a weighing lysimeter of this size, being similar to the dollar cost in 1988 of the large weighing lysimeters at Bushland, Texas (Marek et al., 1988) and actually less expensive in inflation-adjusted dollars. The lysimeter performance is close to expected resolution and accuracy values and is entirely adequate for the intended crop water use research. Preliminary data show that the lysimeter and associated weather instrumentation are working as expected and are able to detect half-hourly changes in weather and associated ET rate responses. In conjunction with use of the NMM in supporting experiments, future research will be aimed at improving knowledge of water use of the major irrigated crops in the JRV and its response to agronomic practices, row spacings, weather, and crop cover factor. Since 35% of the irrigated area in the JRV is occupied by plastic houses, for which irrigation needs are poorly understood, some future research may involve placing a plastic house over the lysimeter to study the water use under plastic.

REFERENCES

- Allen, R. G., L. S. Periera, D. Raes, and M. Smith. 1998. Crop evapotranspiration: Guidelines for computing crop water requirements. Irrig. and Drain. Paper No. 56. Rome, Italy: United Nations FAO.
- Alpert, P., and B. Getenio. 1988. One-level diagnostic modeling of mesoscale surface winds in complex terrain: Part I. Comparison with three-dimensional modeling in Israel. *Monthly Weather Rev.* 116(10): 2025-2046.
- Barani, G.-H., and M. J. Khanjani. 2007. A large electronic weighing lysimeter system: Design and installation. *J. AWRA* 38(4): 1053-1060.
- Black, T. A., G. W. Thurtell, and C. B. Tanner. 1968. Hydraulic load cell lysimeter, construction, calibration, and tests. *SSSA Proc.* 32(5): 623-629.
- Dugas, W. A., and W. L. Bland. 1991. Springtime soil temperatures in lysimeters in central Texas. *Soil Sci.* 152(2): 87-91.
- Evelt, S. R. 2008. Chapter 3. Neutron moisture meters. In *Field Estimation of Soil Water Content: A Practical Guide to Methods, Instrumentation, and Sensor Technology*, 39-54. S. R. Evelt, L. K. Heng, P. Moutonnet, and M. L. Nguyen, eds.

- IAEA-TCS-30. Vienna, Austria: International Atomic Energy Agency. Available at: www-pub.iaea.org/mtcd/publications/PubDetails.asp?pubId=7801.
- Gorry, P. A. 1990. General least-squares smoothing and differentiation by the convolution (Savitsky-Golay) method. *Anal. Chem.* 62(6): 570-573.
- Hignett, C., and S. R. Evett. 2002. Neutron thermalization. In *Methods of Soil Analysis: Part 4. Physical Methods*. J. H. Dane and G. C. Topp, eds. SSSA Book Series 5. Madison, Wisc.: SSSA.
- Howell, T. A., A. D. Schneider, and M. E. Jensen. 1991. History of lysimeter design and use for evapotranspiration measurements. In *Lysimeters for Evapotranspiration and Environmental Measurements: Proc. Intl. Symp. Lysimetry*, 1-9. R. G. Allen, T. A. Howell, W. O. Pruitt, I. A. Walter, and M. E. Jensen, eds. Reston, Va.: ASCE.
- Howell, T. A., A. D. Schneider, D. A. Dusek, T. H. Marek, and J. L. Steiner. 1995. Calibration and scale performance of Bushland weighing lysimeters. *Trans. ASAE* 38(4): 1019-1024.
- Howell, T. A., S. R. Evett, A. D. Schneider, D. A. Dusek, and K. S. Copeland. 2000. Irrigated fescue grass ET compared with calculated reference grass ET. In *Proc. 4th Decennial Natl. Irrig. Symp.*, 228-242. R. G. Evans, B. L. Benham, and T. P. Trooien, eds. St. Joseph, Mich.: ASAE.
- Marek, T. H., A. D. Schneider, T. A. Howell, and L. L. Ebeling. 1988. Design and construction of large weighing monolithic lysimeters. *Trans. ASAE* 31(2): 477-484.
- Marek, T., G. Piccinni, A. Schneider, T. Howell, M. Jett, and D. Dusek. 2006. Weighing lysimeters for the determination of crop water requirements and crop coefficients. *Applied Eng. in Agric.* 22(6): 851-856.
- Pruitt, W. O., and D. E. Angus. 1960. Large weighing lysimeter for measuring evapotranspiration. *Trans ASAE* 3(2): 13-15, 18.
- Savitsky, A., and M. J. E. Golay. 1964. Smoothing and differentiation of data by simplified least squares procedures. *Anal. Chem.* 36(8): 1627-1639.
- Schneider, A. D., T. A. Howell, A. T. A. Moustafa, S. R. Evett, and W. S. Abou-Zeid. 1998. A simplified weighing lysimeter for monolithic or reconstructed soils. *Applied Eng. in Agric.* 14(3): 267-273.
- Van Bavel, C. H. M. 1961. Lysimetric measurements of evapotranspiration in the eastern United States. *SSSA Proc.* 25(2): 138-141.
- Van Bavel, C. H. M., and L. E. Myers. 1962. An automatic weighing lysimeter. *Agric. Eng.* 43(10): 580-583, 586-588.

